Fission gas release and swelling model of metallic fast reactor fuel

Chan Bock Lee *, Dae Ho Kim, Youn Ho Jung

Korea Atomic Energy Research Institute, Yusung, P.O. Box 105, Taejon, South Korea

Abstract

A mechanistic model of fission gas release and swelling for the U–Pu–10Zr metallic fuel in a fast reactor, GRSIS (Gas Release and Swelling in ISotropic fuel matrix), was developed. Fission gas bubbles are assumed to nucleate isotropically from gas atoms in the metallic fuel matrix since they could nucleate at both the grain boundaries and the phase boundaries, which are randomly distributed inside the grain. Bubbles can grow to larger sizes by gas atom diffusion and coalescence with other bubbles. When bubble density or swelling due to bubbles reaches a threshold value, bubbles are assumed to be interconnected to each other to form an open channel to the external free space and then the fission gases inside the interconnected open bubbles are released instantaneously. During the irradiation, fission gases are successively released through the open bubbles. The GRSIS model was validated by comparison with the irradiation test results of U–Pu–10Zr fuels as well as parametric studies of the key variables in the model. © 2001 Elsevier Science B.V. All rights reserved.

PACS: 28.41.AK; 28.41.Bm

1. Introduction

U–Pu–10Zr metallic fuel is being considered as one of the candidates for the fuel of the KALIMER fast reactor which is under development [1]. The concept of using U–Pu–10Zr fuel in the fast reactor was first developed at ANL (Argonne National Laboratory) and irradiation tests of fuels of various compositions were performed extensively in the EBR-II research reactor [2]. When the U–Pu–10Zr metallic fuel is irradiated around 600°C, fission gas bubbles nucleate and grow at a rate much higher than the ceramic UO_2 fuel, due to the high diffusivity of fission gas atoms in the metallic fuel. Fuel swelling due to the fission gas bubbles could start at about 0.5% burnup after the incubation period and then increase rapidly until fuel gap closure at a burnup is less than 2%. Fig. 1 shows the fractional fission gas release as

a function of the burnup for U–Pu–10Zr fuel irradiated in ANL [3]. Fission gases are released out of the fuel through open channels formed by interconnection of the bubbles at a burnup of 0.5–1.0%. Then, fractional fission gas release increases by up to about 70% and becomes saturated at a burnup of 4–5%.

Many models [4–10] have been developed for fission gas release and swelling behavior of the U–Pu–10Zr metallic fuel for the fast reactor. The model in the LIFE-Metal code [4] is an empirical model, which calculates the fission gas release by a simple function using burnup, porosity and temperature. It does not explicitly consider the fission gas bubbles. STARS [5] and ALFUS [6–8] models consider the bubble formation and growth, based upon a model of the UO_2 fuel. Therefore, it is assumed that fission gases are generated inside the grain and then diffuse to the grain boundaries to nucleate the bubbles or to be absorbed by the bubbles in the grain boundaries. However, in the metallic fuel for the fast reactor, the fission gas bubbles could nucleate at the phase boundaries inside the grain as well as at the grain boundaries. The phase boundaries are distributed quite

---

* Corresponding author. Tel.: +82-42 868 2257; fax: +82-42 863 0565.

E-mail address: cblee@kaeri.re.kr (C.B. Lee).

Nomenclature

a_{b_i}	surface area of a bubble-i (m^2)
a_j	lattice constant of bubble-j in FCC lattice
a_0^2	area occupied by a gas atom at the bubble surface (m^2)
ab_{ii}	jump or transition rate of bubble-i into bubble $i+1$ (atoms/s m^3)
ab_{ij}	integration rate of bubble-i into bubble-j by bubble diffusion (atoms/s m^3)
$atnb_i$	density of gas atom in a bubble-i (atoms/bub-i)
bubble-4i or $b4i$	open bubble to which the closed bubble-i is transformed after being open
C_g	gas atom concentration in the matrix (atoms/m^3)
C_{gb_i}	gas atom concentration as the bubble-i in the matrix (atoms/m^3)
D_{b_i}	diffusion coefficient of bubble-i (m^2/s)
D_g	diffusion coefficient of gas atom (m^2/s)
D_s	surface diffusion coefficient (m^2/s)
D_{s_0}	surface diffusion constant (m^2/s)
E_{bb}	empirical bias factor for bubble diffusion to other bubbles
E_{bb_4}	empirical bias factor for bubble diffusion to open bubbles
E_c	empirical correction constant for bubble jump rate
E_{gb_i}	empirical bias factor for gas diffusion to the bubble-i
F	fission density (fission/s m^3)
$f_{i,i+1}$	transition probability of bubble-i into bubble-$i+1$ by collision with bubble-i
f_s	fractional surface area of a closed bubble after interconnected to the open bubbles
f_{th}	fraction of closed bubbles to be open at the threshold closed bubble swelling
f_v	fractional volume of a closed bubble after interconnected to the open bubble
gab_{ij}	collision or integration rate of bubble-i into bubble-j by radial growth of bubble-i due to gas diffusion to bubble-i (atoms/s m^3)
j_{g_i}	gas atom diffusion to a bubble-i (atoms/bub-i s)
J_{g_i}	gas atom diffusion to bubble-i (atoms/s m^3)
$J_{b_1 nucl}$	bubble-1 nucleation rate(atoms/s m^3)
$k_{b_1 nucl}$	bubble-1 nucleation constant (bub-1/s + atom)
k_{g_i}	gas diffusion constant to bubble-i (m^3/s)
k_{ii}	jump rate constant of bubble-i into bubble-$i+1$ (m^3/s)
k_{ij}	collision or integration constant of bubble-i into bubble-i ($j > i$) (m^3/s)
l_j	distance between bubble-j's
N_{b_i}	bubble-i concentration (bub-i/m^3)
P_{ij}	probability of bubble-i to collide with bubble-j due to radial growth of bubble-i
Q_g	activation energy of gas atom diffusion (cal/gm mole)
Q_s	activation energy of surface diffusion (cal/gm mole)
r_{b_i}	radius of bubble-i (m)
r_{b_i}	bubble radius (m)
S_b	bubble swelling
S_c	swelling by the closed bubbles
S_o	swelling by the open bubbles
S_t	total swelling by the closed and open bubbles
S_b	bubble swelling
Δt	time increment(s)
v_{b_i}	volume of a bubble-i (m^3)
Y	fission yield of gas atoms (atoms/fission)

randomly inside the grain in the U–Pu–10Zr metallic fuel. Therefore, the effect of grain size upon fission gas behavior in the metallic fuel may not be significant, compared with its effect in UO$_2$ fuel.

2. Modelling of fission gas behavior

A schematic diagram of the fission gas bubble nucleation and growth in the metallic fuel is shown in Fig. 2. Fission gas atoms are generated by fission, and then nucleate bubbles or diffuse into bubbles. Fission gas bubbles are assumed to nucleate isotropically from the gas atoms in the metallic fuel matrix, since they can nucleate at both the grain boundaries and the phase boundaries which are randomly distributed inside the grain. Bubbles can grow by the diffusion of gas atoms into them. Bubbles are classified into three classes of bubbles-1, 2 and 3 depending upon their sizes. The open bubbles, which are connected to each other and open to the external free space are defined as a fourth bubble type. Open bubbles are assumed to be of the same type as the closed bubbles. When the closed bubble-i becomes the open bubble, it is assumed to be transformed to bubble-4i.

When fuel matrix swelling due to the closed bubbles reaches a threshold value, it is assumed that a certain fraction of the bubbles are interconnected with each other to make the path connected to the external free space and to become open bubbles. Monte Carlo sim-
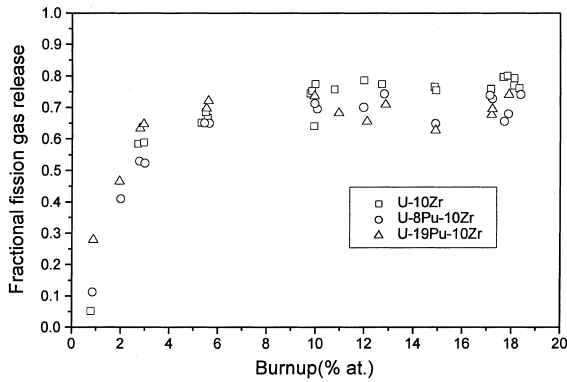
Fig. 1. Fission gas release of ANL fuel irradiation tests [3].

ulations for the relation of the closed bubble swelling, bubble interconnection and open bubble formation based upon the percolation model were performed by Massih [11] for two geometries of the simple cubic (SC) and the simple quadratic (SQ) lattices. For the UO_2 fuel where bubbles nucleate and grow preferentially at the boundaries of the grain, a two-dimensional quadratic geometry needs to be applied. However, when bubbles nucleate isotropically in the matrix of a fuel like the U–Pu–10Zr metallic fuel in the fast reactor, three-dimensional cubic geometry should be applied.

According to the above bubble classification, behavior of fission gas atoms and bubbles can be described as follows.

Bubble-1 is nucleated from the fuel matrix depending upon the gas atom concentrations. Bubble-1 can collide with each other by both diffusion and growth and then grow to bubble-2 with the probability depending upon the difference of the bubble sizes between bubble-1 and bubble-2. Bubble-1 can also collide with bubble-2, 3 or 4 and be absorbed into them.

Bubble-2 can collide with each other and grow to bubble-3 with the probability depending upon the sizes of bubble-2 and bubble-3. Bubble-2 can also collide with bubble-3 or 4 and be incorporated to them. However, when bubble-2 collides with bubble-1, it absorbs bubble-1.

Since bubble-3 is the largest in size among the closed bubbles, their collision with each other does not result in the formation of a higher class of closed bubbles and therefore, bubble-3 is assumed to remain bubble-3 after their collision. The negligence of further growth of bubble-3 by collision with other bubble-3's could be justified by the very low mobility of bubble-3 due to its larger size. However, when bubble-3 collides with bubble-4, the open bubble, it becomes the open bubble. When bubble-3 collides with bubbles-1 and 2, it absorbs them.

The open bubble, bubble-4 consists of bubbles-41, 42 and 43, depending upon the type of the bubble just before it was transformed into an open bubble. Open bubbles are assumed not to move by diffusion and not to grow by gas diffusion since gases in the open bubbles are released out of the fuel.

The diffusion coefficients of the bubbles depend upon bubble size and temperature. Collision of bubble-i with bubble-j due to the radial growth of bubble-i by gas atom diffusion depends upon the amount of radial growth and the distance between bubble-i and bubble-j.

Based upon the percolation theory [11], it is assumed that after volume swelling by closed bubbles such as bubbles-1, 2 and 3 reaches the threshold value, some fractions of bubbles-1, 2 and 3 are interconnected with each other to form the open channel to the external free space, and therefore become the so-called open bubble,
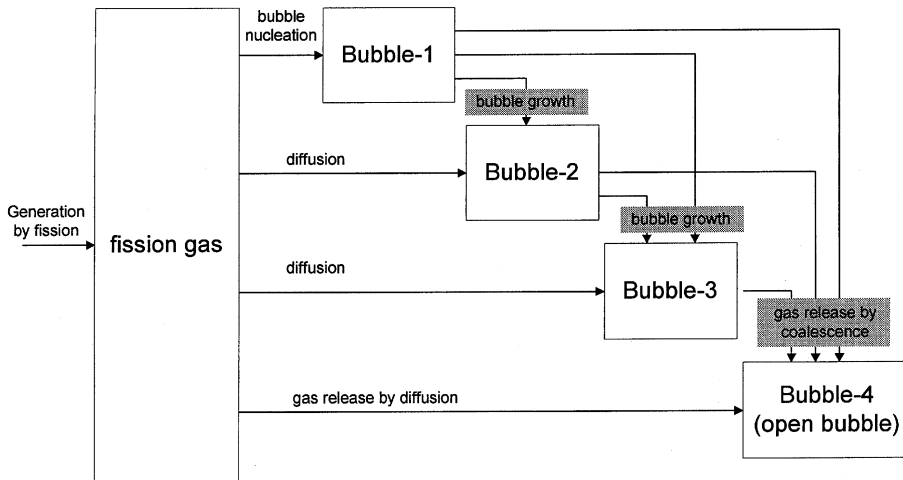

Fig. 2. Fission gas and bubble movement in the GRSIS model.

bubble-4. Fission gases in the interconnected open bubbles are assumed to be released instantly. After threshold bubble swelling, fission gases are successively released through the open bubbles by the diffusion of gas atoms into the open bubbles in the matrix, or the collision of closed bubbles such as bubbles-1, 2 and 3 with open bubbles.

The overall behavior of fission gas atoms and bubbles can be set as follows:

$$\frac{dC_g}{dt} = \text{generation by fission}$$

$$- \text{ gas diffusion to bubbles}$$

$$- \text{ bubble-1 nucleation}, \tag{1}$$

$$\frac{dC_{gb_1}}{dt} = \text{bubble-1 nucleation}$$

$+ \text{ gas diffusion to bubble-1}$

$- \text{ integration of bubble-1 into bubbles-2, 3 and 4}$
by diffusion and growth $- \text{ transition of bubble-1 to}$
bubble-2 after collision with bubble-1 by diffusion and growth $- \text{ instantaneous release by bubble inter-}$
connection at threshold closed bubble swelling, $\quad$ (2)

$$\frac{dC_{gb_2}}{dt} = \text{integration of bubble-1 into bubble-2 by}$$

diffusion and growth $+ \text{ transition of bubble-1 to}$
bubble-2 after collision with bubble-1 by diffusion and growth $+ \text{ gas diffusion to bubble-2} - \text{ integration of}$
bubble-2 into bubbles-3 and-4 by diffusion and growth
$- \text{ transition of bubble-2 to bubble-3 after collision}$
with bubble-2 by diffusion and growth $- \text{ instantaneous}$
release by bubble interconnection at threshold closed bubble swelling, $\quad$ (3)

$$\frac{dC_{gb_3}}{dt} = \text{integration of bubbles-1 and-2 into bubble-3}$$

by diffusion and growth $+ \text{ transition of bubble-2 to}$
bubble-3 after collision with bubble-2 by diffusion and growth $+ \text{ gas diffusion to bubble-3} - \text{ integration of}$
bubble-3 into bubble-4 by diffusion and growth
$- \text{ instantaneous release by bubble interconnection at}$
threshold closed bubble swelling, $\quad$ (4)

$$\frac{dC_{gb_4}}{dt} = \text{gas diffusion into bubble-4} + \text{ integration of}$$

bubbles-1, 2 and 3 into bubble-4 by diffusion and growth $+ \text{ instantaneous increase by bubble inter-}$
connection at threshold closed bubble swelling, $\quad$ (5)

where C_g is the gas atom concentration in the matrix (atoms/m^3) and C_{gb_i} is the gas atom concentration as the bubble-i in the matrix (atoms/m^3).

Then, the balance equations of gas atoms and bubbles can be expressed as follows:

$$\frac{dC_g}{dt} = YF - (J_{g_1} + J_{g_2} + J_{g_3} + J_{g_4}) - J_{b_1 \text{nucl}}, \tag{6}$$

$$\frac{dC_{gb1}}{dt} = J_{b_1 \text{nucl}} + J_{g1} - (ab_{12} + ab_{13} + ab_{14})$$
$$- (gab_{12} + gab_{13} + gab_{14} + gab_{21} + gab_{31})$$
$$- f_{12}(ab_{11} + gab_{11}) - \text{instantaneous release by bubble}$$
interconnection at threshold closed bubble swelling,

$$\tag{7}$$

$$\frac{dC_{gb2}}{dt} = J_{g_2} + ab_{12} + gab_{12} + f_{12}(gab_{11} + ab_{11})$$
$$- (ab_{23} + ab_{24}) - (gab_{23} + gab_{24} + gab_{32})$$
$$- f_{23}(ab_{22} + gab_{22}) - \text{instantaneous release by bubble}$$
interconnection at threshold closed bubble swelling,

$$\tag{8}$$

$$\frac{dC_{gb_3}}{dt} = J_{g_3} + ab_{13} + ab_{23} + gab_{13} + gab_{23} + gab_{31}$$
$$+ gab_{32} + f_{23}(ab_{22} + gab_{22}) - (ab_{34} + gab_{34})$$
$$- \text{instantaneous release by bubble interconnection at}$$
threshold closed bubble swelling, $\quad$ (9)

$$\frac{dC_{gb_4}}{dt} = J_{g_4} + ab_{14} + ab_{24} + aab_{34} + gab_{14} + gab_{24}$$
$$+ gab_{34} + \text{instantaneous increase by bubble}$$
interconnection at threshold closed bubble swelling,

$$\tag{10}$$

where Y is the fission yield of gas atoms (atoms/fission), F is the fission density (fission/s m^3), J_{g_i} is the gas diffusion to bubble-i (atoms/s m^3), $J_{b_1 \text{nucl}}$ is the bubble-1 nucleation rate (atoms/s m^3), ab_{ij} is the integration rate of bubble-i into bubble-j by bubble diffusion (atoms/s m^3), gab_{ij} is the integration rate of bubble-i into bubble-j by radial growth of bubble-i due to gas diffusion to bubble-i (atoms/s m^3) and $f_{i,i+1}$ is the transition probability of bubble-i into bubble-$i+1$ by collision with bubble-i.

The relation of bubble density, N_{b_i} and total gas atom density of bubble-i, C_{gb_i} is

$$C_{gb_i} = atnb_i \cdot N_{b_i}, \tag{11}$$

where $atnb_i$ is the density of gas atom in a bubble-i (atoms/bub-i) and N_{b_i} is the bubble-i concentration (bub-i/m^3).

Collision rate of bubble-i with the open bubbles by diffusion and growth, respectively are:

$$ab_{i4} = ab_{i41} + ab_{i42} + ab_{i43}, \tag{12}$$

$$gab_{i4} = gab_{i41} + gab_{i42} + gab_{i43}. \tag{13}$$

Then, the balance equations of open bubbles are as follows:

$$\frac{dC_{gb_{41}}}{dt} = atnb_1 \cdot \frac{d}{dt} N_{b_{41}}$$
$$= ab_{141} + ab_{142} + ab_{143} + gab_{141} + gab_{142}$$
$$+ gab_{143}, \tag{14}$$

$$\frac{dC_{gb_{42}}}{dt} = atnb_2 \cdot \frac{d}{dt} N_{b_{42}}$$
$$= ab_{241} + ab_{242} + ab_{243} + gab_{241} + gab_{242}$$
$$+ gab_{243} \tag{15}$$

$$\frac{dC_{gb_{43}}}{dt} = atnb_3 \cdot \frac{d}{dt} N_{b_{43}}$$
$$= ab_{341} + ab_{342} + ab_{343} + gab_{341} + gab_{342}$$
$$+ gab_{343}. \tag{16}$$

The specific parameters of gas atoms and bubbles in the above equations can be obtained as follows.

Bubble-1 nucleation rate, $J_{b_1 nucl}$ is obtained from bubble nucleation constant and gas atom concentration in the fuel matrix, such that

$$J_{b_1 nucl} = k_{b_1 nucl} \cdot C_g \cdot atnb_l, \tag{17}$$

where $k_{b_1 nucl}$ is the bubble-1 nucleation constant (bub-1/s atom).

Diffusion of gas atoms into the bubbles can be calculated from the analytical solution in the case that gas atoms diffuse into the spherical sink [12]. Atomic flux into bubble-i by diffusion, J_{g_i} can be calculated as a function of the gas diffusion constant and the concentrations of gas and bubbles are as follows:

$$J_{g_i} = k_{g_i} \cdot C_g \cdot N_{b_i}, \tag{18}$$

$$k_{g_i} = E_{gb_i} \cdot (4\pi r_{b_i}) \cdot D_g, \tag{19}$$

where k_{g_i} is the gas diffusion constant to bubble-i (m^3/s), E_{gb_i} is the empirical bias factor for gas diffusion to the bubble-i, r_{b_i} is the radius of bubble-i (m) and D_g is the diffusion coefficient of gas atom (m^2/s).

The bubble diffusion coefficient can be calculated by a function of surface diffusion coefficient (D_s) and bubble characteristics [12]

$$D_{b_i} = \frac{3a_0^4}{2\pi r_{b_i}^4} D_s, \tag{20}$$

where D_{b_i} is the diffusion coefficient of bubble-i (m^2/s) and a_0^2 is the area occupied by a gas atom at the bubble surface (m^2).

Surface diffusion coefficient, D_s can be obtained by

$$D_s = D_{s_0} \exp(-Q_s/kT), \tag{21}$$

where D_s is the surface diffusion coefficient (m^2/s), D_{s_0} is the surface diffusion constant (m^2/s) and Q_s is the activation energy of surface diffusion (cal/gm mole).

Bubbles can collide with each other by diffusional movement so that collision constant of bubble-i and bubble-j by bubble diffusion, k_{ij} (m^3/s) [12] is

$$k_{ij} = E_{bb} \cdot 4\pi(r_{b_i} + r_{b_j})(D_{b_i} + D_{b_j})$$
$$\cong E_{bb} \cdot 4\pi r_{b_j} \cdot D_{b_i}$$
$$= E_{bb} \cdot 4\pi r_{b_j} \cdot \frac{3a_0^4 D_s}{2\pi r_{b_i}^4}$$
$$= 6E_{bb} \cdot a_0^4 \cdot \frac{r_{b_j}}{r_{b_i}^4} D_s, \quad j > i \text{ and } r_{b_j} \gg r_{b_i}, \tag{22}$$

where E_{bb} is the empirical bias factor for bubble diffusion to other bubbles and k_{ij} is the collision or integration constant of bubble-i into bubble-j (m^3/s).

Then, the integration rate of bubble-i into bubble-j by bubble diffusion ($j > i$) is

$$ab_{ij} = k_{ij} \cdot N_{b_i} \cdot N_{b_j} \cdot atnb_i. \tag{23}$$

When the number density of bubble-i is N_{b_i}, the average distance between bubble-i's can be calculated by assuming FCC (face centered cubic) where there are four bubbles in a cubic lattice [12]. Fig. 3 shows the bubble distribution in a single surface of FCC lattice. The distance between bubbles (l_j) can be calculated from the lattice constant, a_j as $l_j = (\sqrt{2}/2)a_j$. Bubble swelling (S_b) is the total bubble volume in an FCC lattice or total bubble volume per unit volume. Therefore,

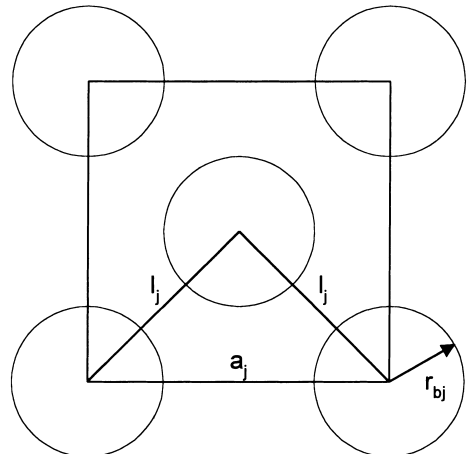$$S_b = \frac{4 \cdot (4/3)\pi r_{b_j}^3}{a_j^3} = N_{b_j} \cdot \frac{4}{3}\pi r_{b_j}^3. \tag{24}$$

Fig. 3. Average distance between the bubbles.

The relation of lattice constant and bubble number density is

$$a_j = \left(\frac{4}{N_{b_j}}\right)^{1/3}. \tag{25}$$

And therefore, the average distance (l_j) between bubbles can be obtained by

$$l_j = \frac{\sqrt{2}}{2} a_j = 1.122 \cdot N_{b_j}^{-1/3}. \tag{26}$$

When there is a bubble-i in the space where bubble-j's are evenly distributed at the number density, N_{b_j} with their distance, l_j as shown in Fig. 4, the average distance between the centers of bubble-i and bubble-j is 0.25 l_j and the distance between the surfaces of bubble-i and bubble-j is $0.25\, l_j - (r_{b_i} + r_{b_j})$. Therefore, the probability of bubble-i colliding with bubble-j due to the radial growth of bubble-i, P_{ij} is

$$P_{ij} = \frac{\text{radial growth of bubble-}i}{\text{distance between the surfaces of bubble-}i \text{ and } j}$$
$$= \frac{\Delta r_{b_i}}{0.25 l_j - (r_{b_i} + r_{b_j})}. \tag{27}$$

The radial growth of bubble-i by gas diffusion to a bubble-i, j_{g_i} can be calculated from the following equations. The volume increase (Δv_{b_i}) and radial growth (Δr_{b_i}) of a bubble-i by gas diffusion are:

$$\Delta v_{b_i} = j_{g_i} \cdot \frac{v_{b_i}}{atnb_i} \cdot \Delta t, \tag{28}$$

$$\Delta r_{b_i} = \frac{\Delta v_{b_i}}{4\pi r_{b_i}^2} = \frac{r_{b_i} j_{g_i} \Delta t}{3 atnb_i}, \tag{29}$$

where j_{g_i} is the gas atom diffusion to a bubble-i (atoms/bub-i s), V_{b_i} is the volume of a bubble-i (m³) and Δt is the time increment (s). Then, collision or integration rate of
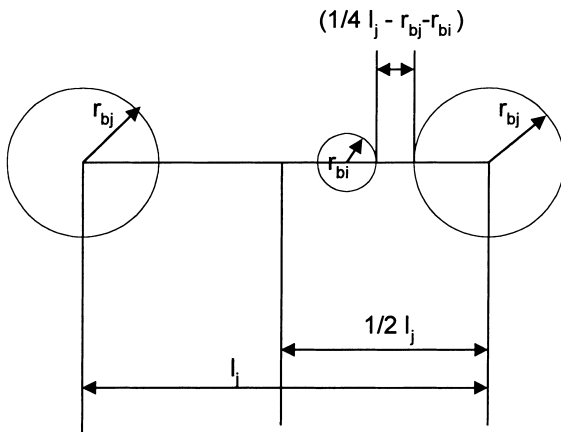
bubble-i with bubble-j by radial growth of bubble-i, gab_{ij} (atoms/s m³) can be calculated by

$$gab_{ij} = P_{ij} \cdot atnb_i \cdot N_{b_i}. \tag{30}$$

Jump or transition rate of bubble-i into bubble-$i+1$ after the collision with bubble-i can be obtained by

$$ab_{ii} = k_{ii} \cdot N_{b_i}^2 \cdot 2 atnb_i, \tag{31}$$

where ab_{ii} is the jump or transition rate of bubble-i into bubble $i+1$ (atoms/s m³) and k_{ii} is the jump rate constant of bubble-i into bubble-$i+1$ (m³/s).

Jump rate constant of bubble-i into bubble-$i+1$, k_{ii} (m³/s) is

$$k_{ii} = E_c \cdot 4\pi \cdot 2 r_{b_i} \cdot 2 D_{b_i} \cdot f_{i,i+1}$$
$$= 24 \cdot E_c a_0^2 \frac{D_s}{r_{b_i}^3} f_{i,i+1}, \tag{32}$$

where E_c is the empirical correction constant for bubble jump rate and $f_{i,i+1}$ is the transition probability of bubble-i into bubble-$i+1$ by collision with bubble-i, $f_{i,i+1}$ can be obtained by

$$f_{i,i+1} = \frac{2 atnb_i}{atnb_{i+1}}. \tag{33}$$

When a bubble-i is incorporated into the open bubbles, it is assumed to become the open bubble-$4i$. After absorption of bubble-i by the open bubble, gases in the bubble-i are assumed to be released into free space which has a lower pressure than bubble-i and therefore, the surface area and volume of bubble-i may decrease as illustrated in Fig. 5. Therefore, when a bubble-i becomes the open bubble, its volume and surface area may be reduced to certain fractions of the initial values such as f_v and f_s, respectively.

Therefore, from Eq. (23), the volume, V_4 and surface area, A_4 of the open bubbles, bubble-4 can be calculated by:

$$\frac{dV_4(t)}{dt} = f_v N_{b_4} (k_{14} N_{b_1} v_{b_1} + k_{24} N_{b_2} v_{b_2} + k_{34} N_{b_3} v_{b_3}), \tag{34}$$

$$\frac{dA_4(t)}{dt} = f_s N_{b_4} (k_{14} N_{b_1} a_{b_1} + k_{24} N_{b_2} a_{b_2} + k_{34} N_{b_3} a_{b_3}). \tag{35}$$

Total swelling by the closed bubbles, S_c is

$$S_c = V_1 + V_2 + V_3. \tag{36}$$

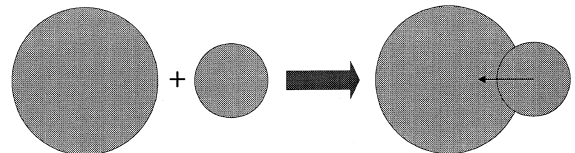Fig. 4. Average distance between surfaces of the bubble-i and bubble-j's.

Fig. 5. Illustration of bubble coalescence.

Total volume of bubble-i, V_i is

$$V_i = v_i N_{b_i} = \frac{4}{3} \pi r_{b_i}^3 N_{b_i} \quad (i = 1, 2, 3). \tag{37}$$

When the swelling by the closed bubbles reaches the threshold swelling (S_{th}) for bubble interconnection to be open to the external free space, a certain fraction of the bubbles become the open bubbles instantaneously. Therefore, when $S_c \geqslant S_{th}$, volume and surface area of the closed and open bubbles change as follows:

$$V_i \rightarrow (1 - f_{th})V_i, \quad i = 1, 2, 3,$$
$$V_4 = f_{th} f_v (V_1 + V_2 + V_3). \tag{38}$$

$$A_i \rightarrow (1 - f_{th})A_i, \quad i = 1, 2, 3,$$
$$A_4 = f_{th} f_s (A_1 + A_2 + A_3), \tag{39}$$

where f_s is the fractional surface area of a closed bubble after interconnected to the open bubbles, f_{th} is the fraction of closed bubbles to be open at the threshold closed bubble swelling and f_v is the fractional volume of a closed bubble after interconnected to the open bubbles.

Total swelling by the closed and open bubbles is

$$S_t = S_c + S_o = V_1 + V_2 + V_3 + V_4. \tag{40}$$

Then, fission gas release (FGR) can be calculated as follows:

$$\text{FGR} = 0, \quad S_t < S_{th}$$
$$= f_{th}(C_{gb_1} + C_{gb_2} + C_{gb_3}), \quad S_t = S_{th}$$
$$= C_{gb_4}, \quad S_t > S_{th}. \tag{41}$$

According to the Monte Carlo simulation of percolation theory for SC lattice geometry, the critical concentration of bubbles (P_c) is 0.32 and the fractional volume of the bubbles (V_{SC}) is 0.17 [11]. Then, the critical swelling for the interlinked tunnel formation by bubble interconnection is calculated as follows:

$$\left(\frac{\Delta V}{V} \right)_{SC} = \frac{V_{SC}}{1 - V_{SC}} = 0.2. \tag{42}$$

Critical swelling in SC lattice geometry is independent of the size of bubble and lattice constant. When P_c is 0.32 in SC lattice geometry, the fraction of bubbles in the largest cluster, that is, the open bubbles, F_{SC}^∞ is about 0.54 [11]. The above calculation is based upon a random distribution of bubbles which are of the same size and sphere shape. Therefore, critical swelling and fraction of bubbles in the largest cluster may change depending upon variations in size and shape of bubbles.

Calculation flow of the GRSIS (Gas Release and Swelling in ISotropic fuel matrix) program [13] is shown in Fig. 6. Bubbles are classified in terms of radius, surface area, volume and atomic density. Bubble sizes should be selected from the microstructure analysis of the irradiated fuels. Threshold swelling and fraction of interconnected bubbles at the threshold swelling need to be set. The next step is reading of the irradiation history, such as time, fission rate and temperature. From the irradiation condition of the fuel, rate constants of the fission gas and bubble movements are calculated. Then, concentrations of gas atoms and bubbles are calculated. Bubble swelling is calculated from the bubble concentrations and threshold swelling for bubble interconnection to be open to the external open space is checked. Then, the fuel gap closure by fuel swelling is checked. When the fuel swelling becomes larger than the fuel gap allowance, bubble swelling is recalculated after increasing the contact pressure between fuel and cladding. As the contact pressure increases, fuel swelling by bubbles decreases. Therefore, it is iterated until fuel swelling is equal to the fuel gap allowance and then, the contact pressure is determined.

Input variables in the GRSIS model are fuel design parameters, a set of bubble characterizations, threshold bubble swelling and a fraction of interconnected bubbles and irradiation histories such as time, fission density and temperature. Then, the output of the GRSIS model is gas atom concentrations in the matrix, concentrations of bubbles, swelling by closed and open bubbles, fission gas release and contact pressure between fuel and cladding.

3. Model evaluation

Table 1 shows the reference data of the variables upon which evaluation of the GRSIS model is based. Fig. 7 shows the general swelling behavior of the fuel irradiated at 550°C as predicted by the GRSIS model. Fuel swelling by the solid fission products increases linearly with the burnup [2]. After some incubation time, the swelling by closed bubbles starts to increase and at the threshold swelling, the open bubbles are assumed to form instantaneously in the GRSIS model.

When total fuel swelling reaches the allowable limit due to gap closure, the contact stress between the fuel and the cladding starts to increase with the burnup. During this period, swelling by closed bubbles decreases due to increase in external pressure on the closed bubble while fraction of open bubbles increases. When the contact stress reaches the yield stress of the porous fuel, fuel deformation occurs while the contact stress is not changed. Fuel deformation occurs by collapse of open bubbles and therefore, the fraction of open bubbles decreases during this period while the fraction of closed bubbles increases since the contact stress does not increase anymore due to fuel deformation. When all the open bubbles have collapsed due to fuel deformation, fuel is allowed to expand or slide in an axial direction
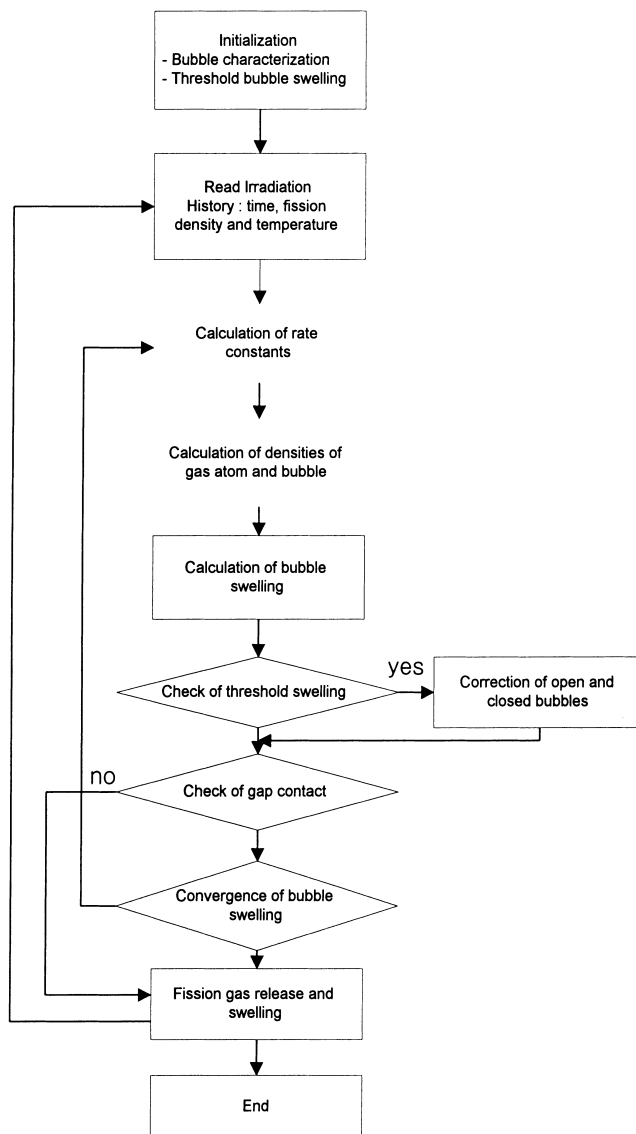
Fig. 6. Calculation flow of the GRSIS model.

since the radial constraint stress from the cladding is higher than the yield stress of the porous fuel.

Fig. 8 compares the fractional fission gas release versus the burnup with the measured data from the irradiation tests of U–10Zr, U–8Pu–10Zr and U–19Pu–10Zr fuels [3]. There is not much difference among the different fuels. In calculations by the GRSIS program, the fuel temperature was assumed to be 550°C during the irradiation. It can be seen that the GRSIS model could predict the general behavior of the metallic fast reactor fuels, even though anisotropic swelling of U–(Pu)–Zr fuel at low temperature such as cavitational void swelling [10] is not considered in the GRSIS model.

Parametric study of the key variables in the GRSIS model was performed as follows.

3.1. Diffusion coefficient of fission gas atoms

There are several correlations available for the diffusion coefficients of the elements in the uranium alloy fuel [7,14,15]. However, there still exists a large difference among the correlations, as much as a factor of $10 \sim 100$. In the GRSIS model, Adda's correlation for U–10Zr fuel [14] is used. Then, the surface diffusion coefficient of the gas atoms was assumed to be larger than the matrix diffusion coefficient of the gas atoms by

Table 1
Reference data of the GRSIS variables for U–PU–10Zr fuel

Class	Variables	Value
Bubble characteristics	Radius of bubble-1 (r_{b_1}, μm)	0.5
	Radius of bubble-2 (r_{b_2}, μm)	2.5
	Radius of bubble-3 (r_{b_3}, μm)	12.5
	Surface tension (N/m)	1.0
Diffusion related constants [14,15]	Gas diffusion factor (D_{go}, m^2/s)	9.5×10^8
	Activation energy of gas diffusion (Q_g, cal/gm mole)	32,000
	Surface diffusion factor (D_{s_0}, m^3/s)	9.5×10^5
	Activation energy of surface diffusion (Q_s, cal/gm mole)	32,000
	Area occupied by surface molecule (a_0^2, m^2)	9×10^{-20}
	Bubble-1 nucleation constant ($k_{b_1 nucl}$, bub-1/s atom)	1×10^{-20}
	Bias factor of gas diffusion to closed bubble (E_{gb_i}, $i = 1, 2, 3$)	1.0
	Bias factor of gas diffusion to open bubble (E_{gb_4})	1.0
	Bias factor of bubble diffusion to closed bubble (E_{bb})	1.0
	Bias factor of bubble diffusion to open bubble (E_{bb_4})	1.0
Threshold swelling	Threshold closed bubble swelling (S_{th})	0.2
	Fraction of interconnected bubbles at threshold swelling (f_{th})	0.3
	Correction factor of bubble volume after becoming open bubble (f_v)	1.0
	Correction factor of bubble surface area after becoming open bubble (f_s)	0.6

a factor of 10^3 [12]. Fig. 9 shows the fission gas release and bubble swelling behavior when the gas diffusion coefficient is changed while the temperature is fixed. When the diffusion coefficient is changed by a factor of 100, there is no significant change in fission gas release behavior, which means that when the gas diffusion coefficient is greater than a certain value, it does not further enhance the fission gas release and swelling. However, when the gas diffusion coefficient is reduced,

bubble swelling rate decreases so that fission gas release by bubble interconnection occurs at higher burnup.

3.2. Temperature

Fig. 10 shows the dependence of fission gas release upon temperature. The bubble swelling rate increases with temperature so that bubble interconnection occurs at lower burnup. However, at temperatures higher than
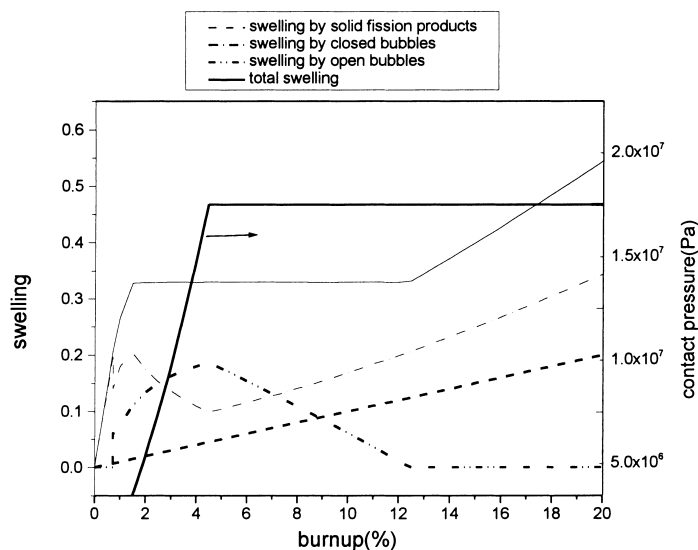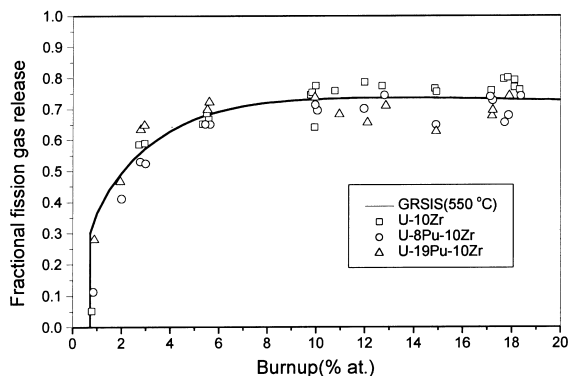

Fig. 7. Fuel swelling and the contact pressure.

Fig. 8. Comparison of the GRSIS prediction with the ANL fuel irradiation test results [3].

about 450°C, there was not much dependence of the threshold burnup and fission gas release upon temperature, so that bubble swelling rate does not increase much with temperature. Temperature dependence is significant only at low temperatures due to the low diffusion coefficients of the gas atoms. As the temperature increases, the fraction of the closed bubbles of larger sizes increase as well as the open bubbles. That is, bubble growth and interconnection are more active at high temperatures. At temperatures less than 300°C, bubble swelling is so low that bubble interconnection and fission gas release do not occur.

3.3. Bubble nucleation rate

Fig. 11 shows the effect of the bubble-1 nucleation rate. In the temperature region where bubble growth and gas diffusion are active, there is no significant effect of bubble nucleation on bubble swelling and fission gas release. Once the bubble is formed in the fuel matrix, the controlling parameter is not bubble nucleation, but the growth of the larger size bubbles.

As to the fission density, there is no significant effect of fission density on the fuel swelling and fission gas release behavior. Even though the gas concentration in the matrix increases slightly with the fission density, the fraction of gas atoms in the fuel matrix is very small compared with those in the bubbles.

3.4. Threshold swelling at bubble interconnection

Fig. 12 shows the effect of threshold swelling at bubble interconnection and the fraction of the bubbles interconnected to be open to the external free space at the point of threshold swelling. As the threshold swelling increases, the burnup at which the instantaneous fission gas release by interconnection of the closed bubble occurs increases. However, after the threshold burnup, there is not much difference in fission gas release. Fractional fission gas release increases with the fraction of the interconnected bubbles at the threshold bubble swelling.

3.5. Classification of bubble sizes

In the GRSIS model, the closed bubbles are divided into three classes depending upon their sizes. The size of bubble-1 represents the minimum size of the stabilized bubbles after nucleation. Bubble-3 represents the maximum possible size of the closed bubbles grown in the fuel matrix before being open to the external space by interconnection to the open bubbles. Therefore, the sizes of bubble-1 and bubble-3 should be determined from the

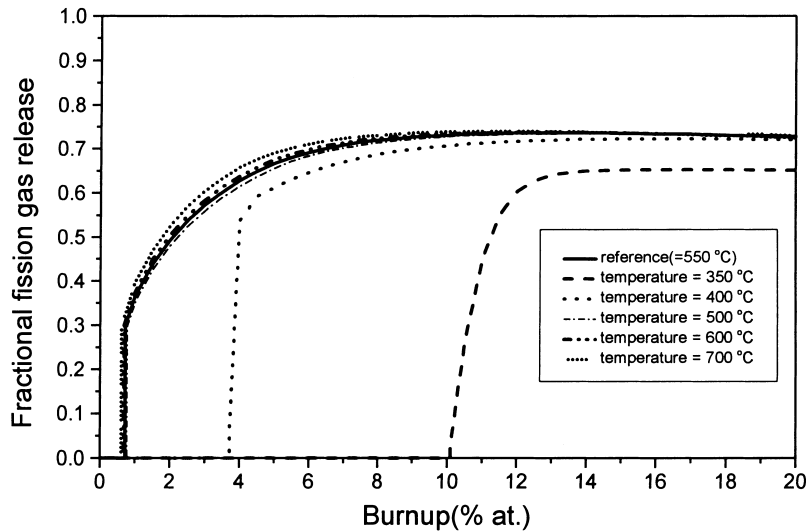Fig. 9. Effect of diffusion coefficient upon the fractional fission gas release.

Fig. 10. Effect of temperature upon the fractional fission gas release.

microstructure examination of the irradiated fuels [16,17]. Then, the size of bubble-2 need to be set in the middle of bubble-1 and bubble-3. However, the well-characterized data on bubble size distribution from the irradiated fuels to determine the reliable bubble size distribution are not available so that the sensitivity analysis of bubble size classification was performed.

Fig. 13 shows the effect of bubble classification upon the fuel behavior. Fuel swelling and fission gas release are slightly dependent upon the difference between bubbles-1, 2 and 3. As the size of bubble-1 decreases, the burnup at threshold swelling increases. As the sizes of bubbles-2 and 3 decrease, fractional fission gas release increases due to easier growth of bubble-1 to bubbles-2 and 3, and subsequent bubble interconnection. It seems that classification of bubbles-1, 2 and 3 with the radii of 0.5, 2.5 and 12.5 μm, respectively, are best fitted to the results of the ANL metallic fuel irradiation tests [3], even though anisotropic swelling of the metallic fuel at the low temperature region such as cavity swelling [10] is not considered in the GRSIS model.

3.6. Fuel gap allowance for swelling

Fig. 14 shows the effect of fuel gap allowance for swelling upon fuel behavior. As the fuel gap allowance
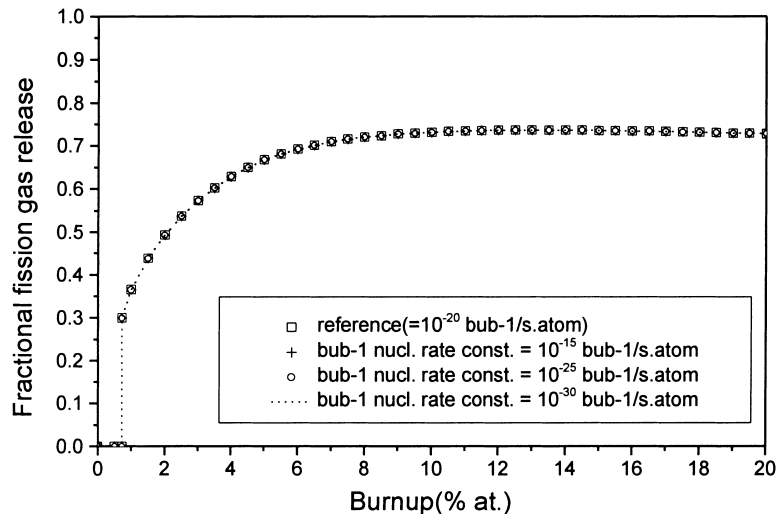

Fig. 11. Effect of bubble nucleation rate upon the fractional fission gas release.
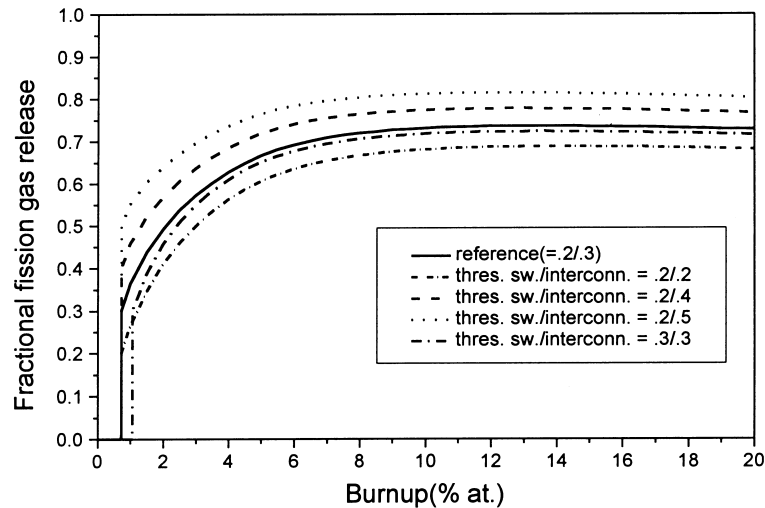
Fig. 12. Effect of threshold swelling and interconnected bubble fraction upon the fractional fission gas release.

for swelling increases, fractional fission gas release increases due to higher allowable fuel swelling before gap closure, while the contact pressure between fuel and cladding decreases. However, fuel behavior before fuel gap closure is not affected by fuel gap allowance for swelling.

3.7. Volume and area reduction of the open bubble

When closed bubbles collide with open bubbles to become open bubbles, the volume and surface area of the closed bubbles may decrease as illustrated in Fig. 5. Fig. 15 shows the effect of the volume and area reduction

of closed bubbles after becoming open bubbles. As volume and area of closed bubbles decrease after they become open bubbles, fractional fission gas release and open bubble swelling decrease.

3.8. Biased diffusion of fission gas atoms to the open bubble

Fig. 16 shows the effect of biased diffusion of gas atoms into the open bubbles. When diffusion of gas atoms to open bubbles is assumed to be two times higher than that to closed bubbles, fractional fission gas release increases by about 8%.
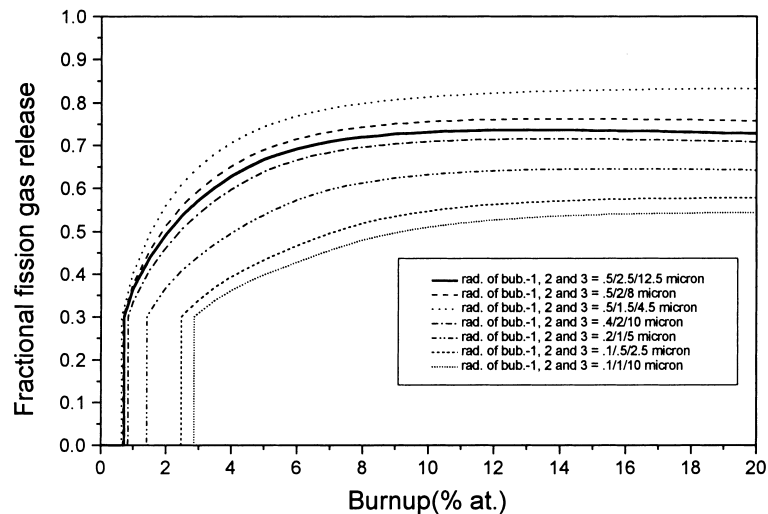

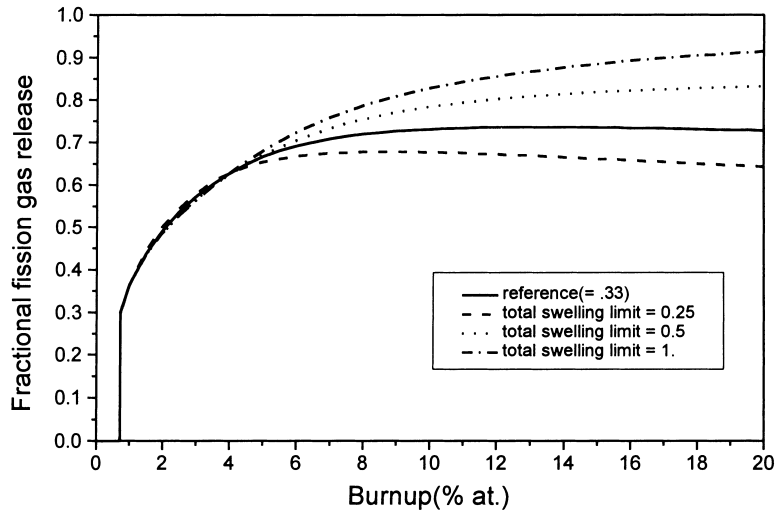Fig. 13. Effect of bubble size classification upon the fractional fission gas release.

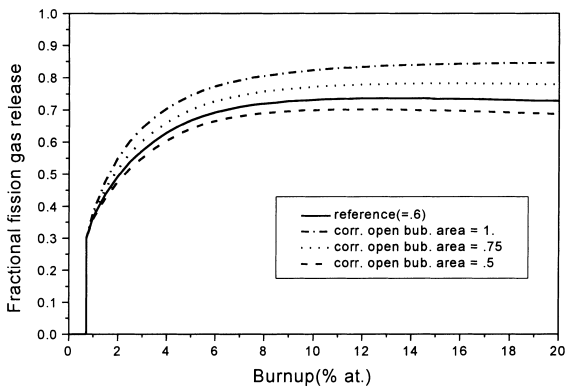Fig. 14. Effect of fuel gap allowance for swelling upon the fractional fission gas release.

Fig. 15. Effect of surface area correction factor of the open bubble upon the fractional fission gas release.
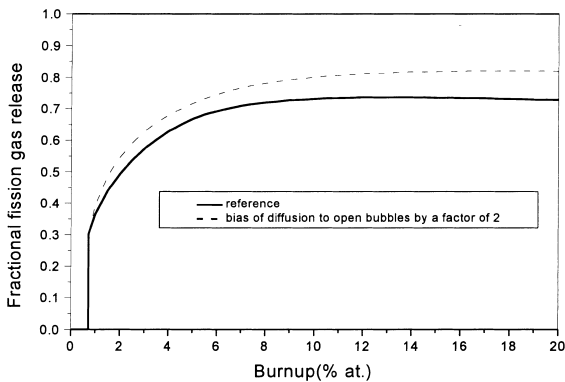

Fig. 16. Effect of biased diffusion to the open bubbles upon the fractional fission gas release.

4. Conclusion and discussion

A mechanistic model of swelling and fission gas release for the U–Pu–10Zr metallic fuel in the fast reactor, GRSIS, was developed. Fission gas bubbles were classified into three classes depending upon their sizes. Bubbles are assumed to nucleate isotropically from the gas atoms in the fuel matrix since the bubbles could nucleate at the phase boundaries which are randomly distributed inside the grain, as well as at the grain boundary. When bubble swelling reaches the threshold value, bubble interconnection could occur to form an open channel to the external free space, and fission gases inside the interconnected bubbles are released instantaneously. The model can also take into account the fuel gap closure caused by fuel bubble swelling.

The GRSIS model was validated by comparison with the irradiation test results in ANL and parametric study of the key variables. It was found that the GRSIS model could predict the general behavior of metallic fast reactor fuels such as U–10Zr, U–8Pu–10Zr and U–19Pu–10Zr, even though anisotropic cavitational void swelling of the fuel at the low temperature region was not considered in the GRSIS model. Parametric study of the GRSIS model showed that fission gas release is very sensitive to the diffusivity of the gas atoms which increases with temperature while it is quite insensitive to grain size, bubble nucleation rate and fission density. However, classification of the bubble sizes and values of the other variables in the GRSIS model may need to be further investigated and verified.

References

[1] C.K. Park, et al., KALIMER Design Concept Report, KAERI/TR-888/97, KAERI, 1997.

[2] G.L. Hofmann, L.C. Walters, T.H. Bauer, Progress Nucl. Energy 31 (1&2) (1997) 83.

[3] R.G. Pahl, D.L. Porter, D.C. Crawford, L.C. Walter, J. Nucl. Mater. 188 (1992) 3.

[4] M.C. Billone, Y.Y. Liu, E.E. Gruber, T.H. Hughes, J.M. Kramer, Status of fuel element modelling codes for metallic fuels, in: International Conference on Reliable Fuels for Liquid Metal Reactors, Tucson, AZ, 1986, p. 5.

[5] J.M. Kramer, T.H. Hughes, E.E. Gruber, Validation of models for the analysis of the transient behavior of metallic fast reactor fuel, in: Transactions of the 10th International Conference on Structural Mechanics in Reactor Technology, 1989.

[6] Y. Tsuboi, T. Ogata, M. Kinoshita, H. Saito, J. Nucl. Mater. 188 (1992) 312.

[7] T. Ogata, M. Kinoshita, H. Saito, T. Yokoo, J. Nucl. Mat. 230 (1996) 129.

[8] T. Ogata, T. Yokoo, Nucl. Technol. 128 (1999) 113.

[9] E.E. Gruber, J.M. Kramer, J. Am. Ceram. Soc. 70 (1987) 699.

[10] J. Rest, J. Nucl. Mater. 207 (1993) 192.

[11] A.R. Massih, J. Nucl. Mater. 119 (1983) 116.

[12] D.R. Olander, Fundamental aspects of nuclear fuel elements, TIC ERDA, 1977.

[13] C.B. Lee, B.H. Lee, C. Nam, D.S. Sohn, GRSIS program to predict fission gas release and swelling behavior of metallic fast reactor fuel , KAERI/TR-1289/99, KAERI, 1999.

[14] Y. Adda, J. Philibert, H. Faraggi, Revue De Metallurgie 54 (1957) 597.

[15] A.D. Schope, L.R. Jackson, Diffusion studies of zirconium–uranium system, Battelle Memorial Inst. Report BMI-T-24, 1950.

[16] G.L. Hofmann, R.G. Pahl, C.E. Lahm, D.L. Porter, Metall. Trans. A 21 (1990) 517.

[17] H. Tsai, A.B. Cohen, M.C. Billone, L.A. Neimark, Irradiation performance of U–Pu–10Zr metal fuels for liquid-metal-cooled reactors, in: Proceedings of the International Conference on Fast Reactor and Related Fuel Cycles, Kyoto, Japan, 1991.